Surfactant-Enhanced Remediation of a Trichloroethene-Contaminated Aquifer. 2. Transport of TCE

DIPAK SAHOO,[†,‡] JAMES A. SMITH,[*,†]
THOMAS E. IMBRIGIOTTA,[§] AND
HEATHER M. MCLELLAN[†,‖]

Program of Interdisciplinary Research in Contaminant Hydrogeology, Department of Civil Engineering, University of Virginia, Charlottesville, Virginia 22903-2442, and U.S. Geological Survey, 810 Bear Tavern Road, Suite 206, West Trenton, New Jersey 08628

Field studies were conducted under an induced gradient in a trichloroethene (TCE)-contaminated aquifer at Picatinny Arsenal, NJ, to study (a) the rate-limited desorption of TCE from aquifer sediments to water and (b) the effect of a surfactant (Triton X-100) on the desorption and transport of TCE. Clean water was injected into the contaminated aquifer for 206 day. Triton X-100 was added for a 36-day period (days 36−71 from the start of clean water injection). The effect of Triton X-100 on the desorption and transport of TCE in the field was examined by observing the concentrations of these two solutes in four monitoring wells 3−9 m from the injection wells. These data show a small but discernible increase in the TCE concentration in two of the wells corresponding approximately to the time when surfactant reaches the wells; in the other two monitoring wells, the increase in TCE concentration is negligible. A solute transport model that assumes local sorption equilibrium and used a laboratory-derived distribution coefficient could not adequately describe TCE desorption and transport observed in the aquifer. Two model formulations that accounted for rate-limited sorption—two-site and multisite models—fit the data well. TCE concentrations after surfactant injection were underpredicted by the models unless mass transfer rate was increased to account for the effect of surfactant on the rate of TCE desorption. The concentration data from the two wells and the model analysis suggest that the rate of TCE desorption is increased (by approximately 30%) as a result of Triton X-100 injection.

Introduction

Releases of organic contaminants, including trichloroethene (TCE), have resulted in groundwater contamination at many sites across the United States. These contaminated sites have resisted cleanup by conventional methods such as pump-and-treat because of the slow rate of pollutant desorption from soil to water (*1−6*), the presence of residual NAPL, and

physical and chemical heterogeneities at the site. In the absence of NAPL or significant physical heterogeneity, slow desorption evidenced by local nonequilibrium is the primary cause of inefficiency in pump-and-treat operations. Several field-scale experiments have shown that the transport of organic compounds in the groundwater is nonequilibrium in nature (*7−13*). In another study, under forced-gradient flow conditions (using an injection−extraction well system), plots of organic solute concentration versus time exhibited extended tailing, suggesting rate-limited transport (*14*).

Nonionic organic solutes primarily partition into soil organic matter (*15*) and undergo slow or rate-limited desorption (*2, 16*). It has been postulated that several different processes cause this sorption-related nonequilibrium. However, many studies have suggested that slow intraorganic matter diffusion may be the primary cause for nonequilibrium sorption in soil−water systems (*17−20*).

Soil organic matter can be envisioned as a three-dimensional matrix of polymer chains with a relatively open, flexible structure (*17*). The diffusional resistance of small solute molecules, such as benzene and TCE, in concentrated polymeric solutions is generally believed to be caused by the tortuous movement of the solute through the polymer matrix (*21*). Over long time periods, changes in water pH, ionic strength, or temperature may cause rearrangement of the alkyl and aryl functional groups in soil organic matter (*22*); this in turn may cause some fraction of the sorbed solute to be "trapped" as diffusional paths are blocked. The rate of desorption varies inversely with the time of exposure to contamination; long-term field-contaminated soils can be expected to exhibit slow desorption.

Surfactants can reduce the water/soil organic matter interfacial tension and cause swelling of the soil organic matter. When the concentration of a solvent in a polymer is increased, the polymer matrix must undergo configurational changes that "swell" or expand the organic polymer medium. The resulting diffusion rate of a small solute molecule in the polymer solution can, thereby, be increased (*20, 23, 24*). Recent laboratory sorption−desorption and transport studies conducted on long-term TCE-contaminated soil found that the nonionic surfactant Triton X-100 was able to cause a modest increase in the desorption rate of TCE (*3*). Another study that investigated the effect of surfactants on the rate of carbon tetrachloride desorption from laboratory-contaminated soil reported that Triton X-100 increases the mass-transfer coefficient of desorption (*18*).

Because there are only a few documented field studies of the transport of organic compounds with kinetic sorption and the effects of surfactant on pollutant transport, additional studies are needed to elucidate this transport process in the field. This work reports the results of a field study that was conducted at a TCE-contaminated aquifer at Picatinny Arsenal, NJ. Since pump-and-treat remediation began at the site in 1992 (Figure 1), there has been no significant decrease in groundwater TCE levels in the aquifer in areas more than 40 m from the withdrawal wells, suggesting that there is resistance to desorption. In this study, the transport of TCE with rate-limited sorption and under an induced gradient in the field is analyzed using a two-site or bicontinuum model (with a single mass-transfer coefficient) and a multisite model (with a distribution of mass-transfer coefficients). Additionally, the effect of Triton X-100 on the transport of TCE in the field is reported here. There are a few reported field studies on the effect of surfactants on the removal of pure, nonaqueous phase organic contaminants from soil (*25*); however, to our knowledge, there is no reported

* To whom correspondence should be addressed; e-mail: jas9e@virginia.edu; telephone: (804)924-7991; fax: (804)982-2951.
† University of Virginia.
‡ Present address: Department of Geology, University of Illinois, Champaign, IL.
§ U.S. Geological Survey.
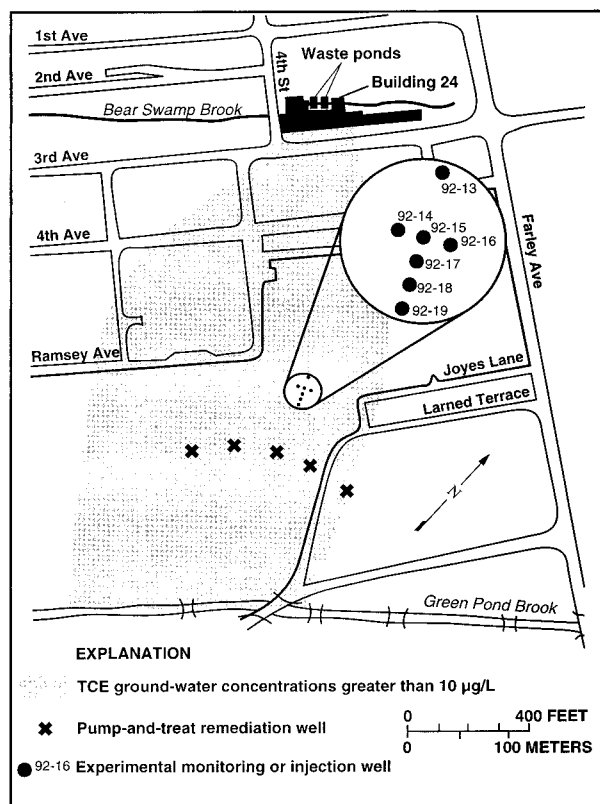‖ Present address: Woodward-Clyde, Inc., Blue Bell, PA.

FIGURE 1. Map of the field site, Picatinny Arsenal, NJ, showing the location of the injection and monitoring wells, the pump-and-treat withdrawal wells, and the region of trichloroethene-contaminated groundwater.

field study using a surfactant to increase the desorption rate of TCE or other organic compounds. This paper is the second of a two-paper series addressing the results of a field test of surfactant-enhanced aquifer remediation at Picatinny Arsenal, NJ. The first paper (26) focused on the transport of a nonionic surfactant, Triton X-100, through the unconfined, TCE-contaminated aquifer at the site. The objectives addressed in this paper are (a) to demonstrate the ability of surfactant to enhance TCE desorption from sediment in a contaminated aquifer and (b) to test the applicability of the two-site and multisite kinetic models in the field.

Materials and Methods

Materials. Hexane (>99% purity), methanol (>99% purity), and TCE (>99% purity) were obtained from Aldrich and Sigma Chemical Co. Triton X-100, a nonionic heterogeneous octylphenol ethoxylate surfactant, was obtained from Union Carbide Chemical and Plastics Technology Corp. The average molecular weight is 628. From laboratory measurement of surface tension at various concentrations of Triton X-100, the critical micelle concentration (cmc) was found to be 130 mg/L.

Description of Field Site. Picatinny Arsenal (Figure 1) is located in a narrow, glaciated valley in north-central New Jersey atop 50−65 m of stratified and unstratified drift, which in turn overlies a weathered bedrock surface. Three major hydrogeologic units are formed from the unconsolidated sediments at the site: a 15−21 m thick unconfined sand-and-gravel aquifer; an 8−21 m thick confining layer composed of fine sand, silt, and clay; and an 8−35 m thick confined sand-and-gravel aquifer (27). The water table is 2−4 m below land surface over most of the study area (4). The approximate direction of groundwater flow in the unconfined aquifer is from Building 24 to Green Pond Brook (Figure 1). The

horizontal hydraulic conductivity, K, in the unconfined aquifer ranges from 0.0001 to 0.0013 m/s, and average groundwater velocities range from 0.3 to 0.9 m/day (1, 28).

From 1960 to 1983, Building 24 (Figure 1) was used for metal plating, cleaning, and degreasing operations. TCE was the primary solvent used for degreasing. Because of improper disposal practices, a plume of TCE-contaminated groundwater developed in the unconfined aquifer from Building 24 to Green Pond Brook (Figure 1). Over the past decade, several other studies have thoroughly characterized the site hydrogeology and contamination (1, 4, 27, 29−32). During the installation of the seven monitoring and injection wells, soil cores were collected from the study area by hollow stem augering. These soil cores were composited for use in laboratory studies.

Field Experimental Methods. The transport of TCE at the field site was studied using an array of seven 5 cm diameter poly(vinyl chloride) injection and monitoring wells installed approximately in the center of the contaminant plume (Figure 1). In this region, the unsaturated zone is approximately 3.3 m thick, and the unconfined aquifer extends from a depth of 3.3 m to a depth of 16.2 m. Wells 92-14, 92-15, and 92-16 were used as injection wells and are screened from a depth of 9.7−16.2 m. Wells 92-13, 92-17, 92-18, and 92-19 are monitoring wells and are screened from a depth of 12.2−13.8 m. Each of the wells are 3.1 m away from the closest well except well 92-13, which is 9.3 m north of the injection wells. The hydraulic conductivity of the study area determined by a series of slug tests ranged from 1.02×10^{-5} to 1.62×10^{-4} m/s (26).

From May 23, 1995 (day 1), to December 26, 1995 (day 217), water (from Picatinny Arsenal drinking water supply) was injected into wells 92-14, 92-15, and 92-16 at rates of 2.0, 26.5, and 15.0 L/min, respectively. These injection rates resulted in approximately equal steady-state hydraulic heads for wells 92-14 (211.49 m) and 92-16 (211.32 m) and a slightly higher hydraulic head for well 92-15 (211.69 m). The relatively low injection rate in well 92-14 needed to produce a hydraulic head roughly equal to the heads in the other two injection wells probably reflects some clogging of the well screen or a lower local hydraulic conductivity. This observation is supported by the slug-test results (provided in ref 26). On June 3, 1995 (day 12), 20 L of water containing 7.5 kg of KBr (250 g/L Br$^-$) was injected into well 92-15 over a 20-min period. From June 28, 1995 (day 36), to August 2, 1995 (day 71), water discharged into injection well 92-15 contained Triton X-100 at a concentration of 400 mg/L at 26.5 L/min.

Water samples were collected in airtight glass bottles with Teflon-lined caps and zero headspace and were analyzed at an on-site laboratory for TCE, Triton X-100, and Br$^-$. The samples were analyzed for TCE by purge-and-trap capillary column gas chromatography with a flame ionization detector. An anti-foaming agent, Dow Corning Antifoam 1510, was used to prevent foaming in the purge-and-trap process, which results from the presence of surfactant in the aqueous samples. The concentration of Triton X-100 in groundwater samples was determined by a spectrophotometric method (26, 33, 34). The concentration of Br$^-$ in groundwater samples was determined using an Orion specific ion electrode and a double junction reference electrode.

Laboratory Experimental Methods. A batch equilibration method was used to determine the equilibrium distribution coefficient of TCE between water and the field soil. Prior to use in these batch experiments, TCE in the soil was removed by heating the soil sample for 48 h at 105 °C; the soil was analyzed after incubation, and no TCE was detected. Clean soil (6.0 g) and water or surfactant solutions (12 mL) containing different amounts of TCE were added to 15-mL centrifuge tubes. After 3 day of shaking at 15 °C, the aqueous

TCE concentration was measured. The partition coefficients (K_d) were obtained by fitting a linear isotherm model to the data; the K_d of the soil−water system was found to be 0.09 L/kg. The organic carbon content in the soil (f_{oc}) was 0.1%, which implies that the organic carbon-normalized partition coefficient, K_{oc}, for TCE is 90 L/kg, which compares well to previously measured K_{oc} values for Picatinny Arsenal soil (4). To obtain the initial soil-phase concentration of TCE, drilling cores were analyzed. Analysis of the soil for TCE was done using a hot-methanol extraction (4, 35).

Solute Transport Simulations

Model Setup. Steady-state flow and transient solute transport were assumed. The flow was assumed to be 2-D, with constant head boundaries at the upper (northern) and lower (southern) boundaries and no flow boundaries on the side boundaries far away from the injection wells. There is some vertical flow close to the injection well as water is not injected uniformly throughout the depth of the aquifer. However, a few feet away from the injection wells the flow should approximate horizontal flow. For TCE transport, a zero-concentration gradient boundary condition was assumed at all boundaries, which were away from the region of interest. Since the concentration gradient and the flow velocity are high at the injection wells, a finer mesh was used in that region. Also, the time step was allowed to increase with time (details of the model setup are provided in ref 26).

The initial condition of the TCE in the aquifer was determined by collecting water samples from the seven wells before the start of injection of water into the aquifer. The initial average aqueous-phase concentration was 2840 μg/L. Concurrent to this study, the soil-phase TCE concentration was measured by the U.S. Geological Survey (Dr. Timothy Wilson, written communication, 1996) on soil cores collected at various depths in the proximity of the test area. The average TCE concentration in soil at depths of 10−15 m was 800 μg/kg. The average TCE concentrations in soil and water were used as uniform initial conditions.

The results of the Br^- test were used to calibrate the groundwater flow part of the simulation as well as the dispersivity. The groundwater flow moved north and south from the injection wells. The aquifer hydraulic conductivity and porosity were determined to have a value of 1.3×10^{-4} m/s and 0.28, respectively (26). From the flow and tracer data modeling, spatially variable dispersivity was suggested; the dispersivity values were found to increase from 0.08 to 1.04 m with distance away from the injection wells (26). The ratio of longitudinal to lateral dispersivity was assumed to be equal to 10.

Parameter Estimation. A parameter estimation routine using Powell's direction set method (36) was run in conjunction with SUTRA to calibrate the kinetic parameters by minimizing the squared normalized differences between the observed and modeled concentrations. The merit function or error is defined as the sum of the square of the normalized deviation and is mathematically given as

$$\text{merit function (error)} = \sum [(\text{data} - \text{model result})/\text{data}]^2$$

This merit function ensures that the percentage error at each comparison point is given equal weight. Using just the square of the deviation instead of the normalized deviation would result in the model fit being biased in favor of the earlier data points showing higher concentrations.

Several investigators (37−39) have presented models accounting for rate-limited sorption. In this study, the two-site and the multisite sorption models were used to simulate the field experiment. The test site is a fairly homogeneous sand-and-gravel aquifer, and sorption-related nonequilibrium was considered to predominate over physical heterogeneity. SUTRA (40), a two-dimensional finite-element groundwater model, was modified to incorporate the two-site and the multisite sorption models. Both these sorption models assume a linear first-order mass-transfer expression to represent the sorption/desorption from the rate-limited sites.

Two-Site Model. The governing equations incorporating the two-site sorption model are

$$\left(1 + \frac{F\rho K_d}{\theta}\right)\frac{\partial C}{\partial t} + \frac{\rho}{\theta}\frac{\partial S_k}{\partial t} = \nabla\cdot(D\nabla C) - \nabla\cdot(vC) \quad (1)$$

$$\frac{\partial S_k}{\partial t} = k[(1 - F)K_d C - S_k] \quad (2)$$

subject to a zero-concentration gradient at all boundaries and to the following initial conditions:

$$C(x,y,0) = C_i$$

$$S_k(x,y,0) = S_i$$

Here F is the fraction of equilibrium sites, D is the dispersion coefficient, C is the aqueous solute concentration, C_i is the initial measured aqueous TCE concentration, S_i is the initial measured sorbed TCE concentration, v is the linear velocity, ρ is the bulk density, θ is the moisture content or porosity, and S_k is the solute concentration in soil contributed by the solute sorbed in the kinetic site (with a single-valued rate constant, k). The above equations apply to the equilibrium model when $F = 0$.

Multisite model. A γ-probability distribution (5) is used to represent the distribution of kinetic rate constants. A mean rate constant, k, and a coefficient of variation, CV, define the distribution of the γ-density function. The governing equations incorporating the multisite sorption model are as follows:

$$\frac{\partial C}{\partial t} + \frac{\rho}{\theta}\frac{\partial S}{\partial t} = \nabla\cdot(D\nabla C) - \nabla\cdot(vC) \quad (3)$$

$$\frac{\partial S}{\partial t} = \sum_{\kappa = 1}^{NK} k_\kappa[K_d C - S_\kappa] \quad (4)$$

where the subscript κ represents the κth compartment or sorption site, NK is the number of compartments or sites, S_κ is the solute concentration in the soil due to site κ, and S is the total solute concentration in the soil due to all the kinetic sites. NK discrete sites are used to represent the continuous distribution of sites, and each site occupies 1/NK fraction of the soil (an NK of 15 was determined to adequately represent the continuous distribution in this case). The representative mass transfer coefficient, k_κ, for each of the sites is obtained from a γ probability density function (details are provided in ref 5). The initial conditions are

$$C(x,y,0) = C_i$$

$$S_\kappa(x,y,0) = \frac{S_i}{(NK)}$$

for every site, κ.

Results and Discussion

The TCE concentrations in the four monitoring wells are shown in Figures 2−4. Because water was being injected continuously into injection wells 92-14, 92-15, and 92-16,
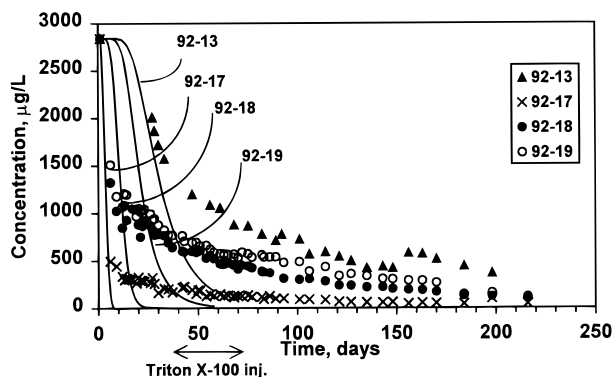
FIGURE 2. Equilibrium transport model prediction of TCE and observed TCE concentrations as a function of time for all the monitoring wells.
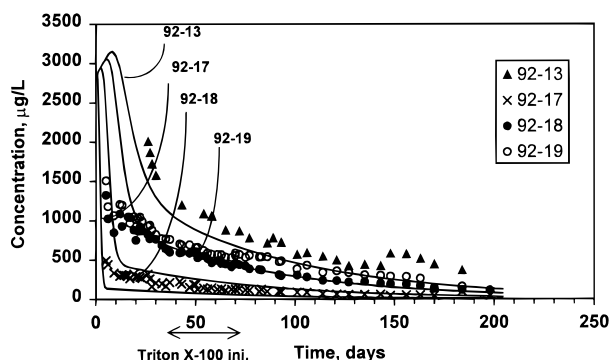

FIGURE 3. Two-site kinetic transport model simulation of TCE for 200 days and observed TCE concentrations for all the monitoring wells
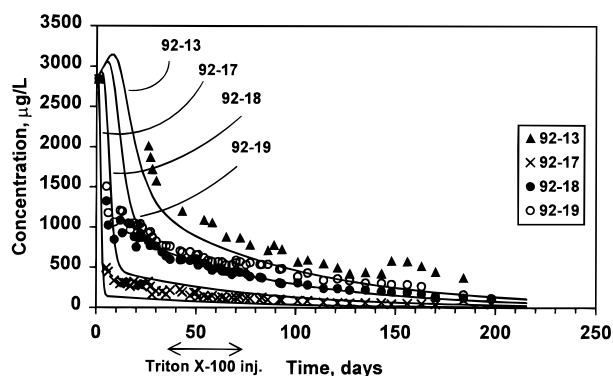

FIGURE 4. Multisite kinetic transport model simulation of TCE for 200 days and observed TCE concentrations for all the monitoring wells.

TCE concentrations in these wells were near zero and are not shown. All the wells show a gradual decreasing trend in TCE concentration resulting from flushing by freshwater. All the TCE concentration curves exhibit extensive tailing, which can be indicative of kinetic desorption from soil and/or physical and chemical flow-field heterogeneities. Because of the regional groundwater flow system, the velocity imposed by the injection is lower northward (relative to southward) from the injection wells. Consequently, the concentration drop in the wells to the south (92-17, 92-18, and 92-19) is greater than that in the well to the north (92-13). The observed TCE concentrations in well 92-19 are similar to those of well 92-18 located 3.1 m closer to the injection wells (Figure 1). These data suggest there are flow heterogeneities including preferential flow pathways in the region between

wells 92-18 and 92-19. Similar results were observed for Triton X-100 and Br$^-$ in these wells (*26*).

Model Results. The transport of TCE is analyzed through model simulation. A uniform hydraulic conductivity and spatially variable dispersivity were assumed for this site. The observed local heterogeneities in the flow system described in the previous section are not incorporated in the simulations because the purpose of this modeling was to investigate the different reactive models and also because of lack of adequate data for K values. Furthermore, some of the physical heterogeneity is accounted for by using spatially variable dispersivities. Three sorption models are examined here: equilibrium, two-site, and multisite.

Equilibrium Sorption Modeling. The equilibrium sorption model was run using the K_d value determined from the laboratory batch sorption experiments described previously (0.09 L/kg). The model prediction is shown in Figure 2 along with the observed concentrations of TCE. Consistent with earlier postulation, the equilibrium sorption model does not fit the data accurately. The predicted concentrations drop rather sharply and underpredict the long-term TCE concentration data observed in all the wells.

Next, the performance of kinetic models is examined. The two-site and the multisite models are studied in this context. In contrast to the equilibrium model, which had no field-calibrated parameters, the kinetic models used in this study each contain two fitting parameters.

Two-Site Modeling. The desorption of TCE from soil, based on prior laboratory evidence, was assumed to be kinetic in nature. The first 200 days of data from all the monitoring wells (92-13, 92-17, 92-18, and 92-19) were fitted by adjusting the two kinetic parameters—the equilibrium site fraction (F) and mass transfer constant (k) (Figure 3). The results show a relatively good overall fit as compared to the fit with the equilibrium model. The fitted values of F and the single kinetic rate constant k were found to be 7.8×10^{-4} and 1.62×10^{-7} s^{-1}, respectively (error = 48.26). The low value of F implies that there are essentially no equilibrium sites and the model is equivalent to a one-site kinetic model.

Multisite Modeling. A multisite kinetic model with a γ-distribution of rate constants was used to represent the sorption−desorption process in the field. The coefficient of variation of the distribution (CV) and the mean kinetic rate constant (k) were varied to fit the model. The first 200 days of data from all the monitoring wells (92-13, 92-17, 92-18, and 92-19) were fitted with a single set of two kinetic parameters: CV and mean mass-transfer constant, k. When the model was fit to the first 200 days of data from the four wells (Figure 4), the system had a mean mass-transfer coefficient of $k = 1.64 \times 10^{-7}$ s^{-1} and a CV of 1.61×10^{-4} (error = 50.32). The results (Figure 4) show that a reasonably good overall fit was achieved as compared to that with the equilibrium model (Figure 2). The closeness of the fit for the multisite model was comparable to that of the two-site model (Figure 3), with a difference in the errors of about 4%.

The small coefficient of variation (CV) of 1.61×10^{-4} suggests that the γ-density function that describes the field sediment has a narrow distribution, tending toward a single mass-transfer coefficient. In the case of the two-site model, all the sites have a single rate constant with virtually no equilibrium sites. The low values of CV and F demonstrate that there is a single rate constant that is applicable, making the two models nearly identical. In fact, a one-site kinetic model can fit the data equally well.

Effect of Surfactant. In this section, the effect of Triton X-100 on TCE desorption and transport is discussed; the transport of the surfactant was reported in a previous paper (*26*). After the flow system reached steady state (by 6 days after the injection of freshwater began), samples were collected for 30 days to establish a TCE concentration profile
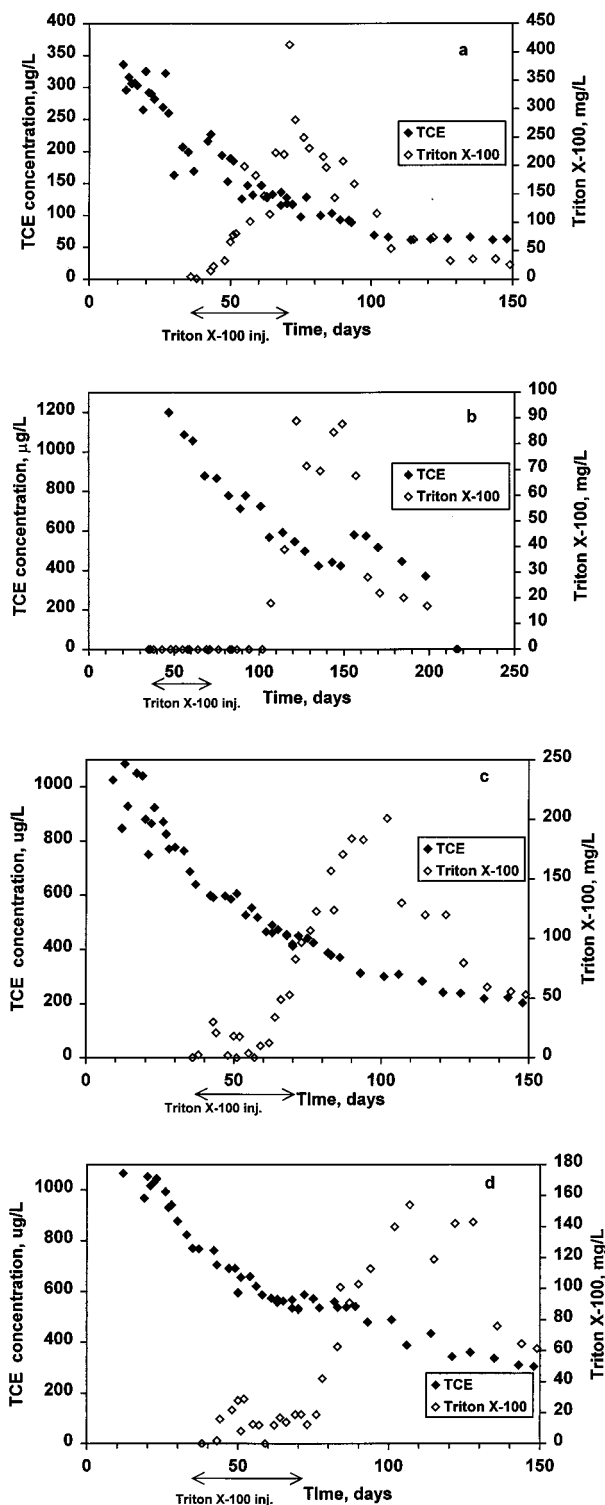
FIGURE 5. Aqueous TCE and Triton X-100 concentrations in monitoring wells: (a) 92-17, (b) 92-13, (c) 92-18, and (d) 92-19.

in the groundwater in the absence of Triton X-100. Triton X-100 (at 400 mg/L) was injected into well 92-15 from day 36 to day 71. The effect of the surfactant on the transport of TCE can be expected to be observed in the monitoring wells sometime after day 36.

The effect of the surfactant on TCE desorption is evident from visual examination of the temporal plots of surfactant and TCE concentrations. Figure 5a shows the plots of TCE and Triton X-100 concentration vs time in well 92-17, which is 3.1 m from the injection well in the regional downgradient

direction. From 5 to 7 days (day 41 to day 43) after Triton X-100 was injected into the groundwater, there is a discernible jump in the TCE concentration. The surfactant was detected in the well around day 42, about 6 days after it was injected. The surfactant interacts with the soil as soon as it is released into the aquifer and affects TCE desorption. Thus, changes in the TCE concentrations in the nearest monitoring well (92-17) should be observed within 2 days (based on groundwater travel time from Br^- tracer test) after the surfactant is released into the aquifer. However, noticeable changes in TCE concentration occur only after 5−7 days of surfactant injection, suggesting that the surfactant front has to spread through a greater portion of the aquifer before the TCE desorption is significantly affected.

Similarly, Figure 5b shows the plots of TCE and Triton X-100 concentration versus time in well 92-13, which is 9.1 m from the injection well. At about day 100 (64 days after surfactant injection began) there is a very small jump in the groundwater TCE concentration, and at about 150 days (114 days after surfactant injection began) there is a marked jump in the groundwater TCE concentration. The surfactant correspondingly reaches the well around day 100 and peaks in the well around day 150. Although the surfactant has reached the well around day 100, its concentration is low and, therefore, does not influence the TCE desorption significantly. An increase in TCE concentration is observed only later, around day 150, when the Triton X-100 concentration has reached a peak of 90 mg/L.

The data in wells 92-18 and 92-19 (Figure 5c,d) did not show increases in the TCE concentration after the surfactant was injected. Some of the changes in concentration may have been small and could have been masked by source dispersion and scatter in the data.

Quantification of the Effect of Triton X-100 on Rate Constant. TCE concentration data from the individual wells were modeled separately to isolate the effect of surfactant on the kinetic sorption parameters. The multisite sorption model was applied (although, the two-site model would have been equally appropriate) for this analysis. The effect of surfactant on the desorption of TCE is most apparent from observation of TCE concentrations in wells 92-13 and 92-17. The observed aqueous TCE concentration data was used to calibrate the two kinetic model parameters, the mean k and CV, for the multisite sorption model. The transport of TCE is complex because its transport is coupled with surfactant transport. Surfactant concentration is a function of space and time. Because the kinetic mass-transfer parameters are related to surfactant concentration, the kinetic parameters are also functions of space and time. Because SUTRA only handles single-solute transport, SUTRA cannot model sorption kinetics and TCE transport in the presence of surfactant accurately.

As an alternative, TCE transport is decoupled from surfactant transport by assuming that, before the Triton X-100 reaches the observation wells, the effect of surfactant on TCE mass transfer is small—that is, the observed TCE concentration in the well is not influenced greatly by Triton X-100. TCE transport is modeled for this period, and the mean k and CV values are calibrated. Using the calibrated k and CV, the model curve is projected beyond this period; this curve approximately predicts the expected TCE concentration profile in the well if no Triton X-100 were present. Comparison between the predicted TCE concentration and the actual data, in this later period, qualitatively illustrates the effect of Triton X-100 on TCE concentrations.

The surfactant took about 100 days to reach well 92-13. First, the model was calibrated to the TCE data in this well during these 100 days, and the CV and the mean mass-transfer coefficient were determined to be 1.92×10^{-4} and $2.64 \times 10^{-7}\ \mathrm{s}^{-1}$, respectively. When the model is projected into the
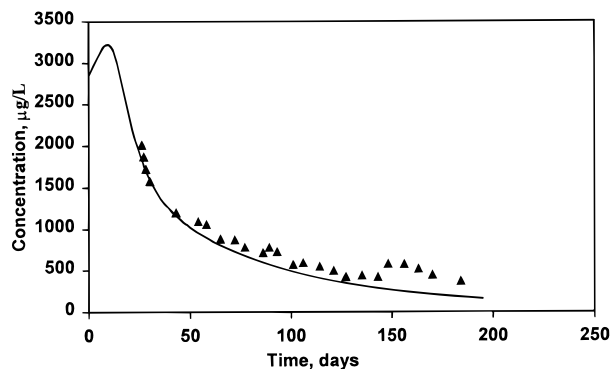
FIGURE 6. Observed and model (multisite) predicted TCE concentrations in well 92-13. The model results are based on kinetic rate parameters obtained from fitting the first 100 days of TCE data.
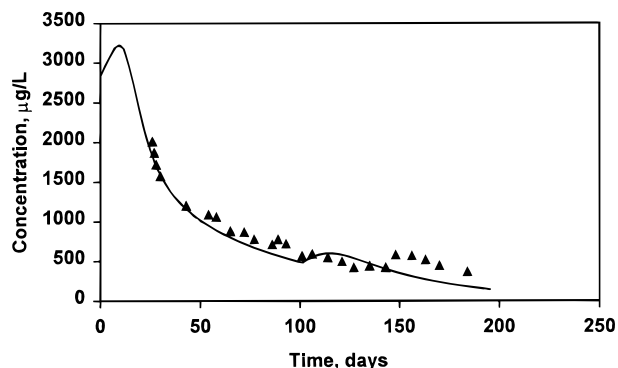

FIGURE 7. Observed and simulated TCE concentrations (using multisite model) in well 92-13 obtained by fitting the data separately for the first 100 days and for the period between 100 and 200 days.

next 100 days using these parameters, the model underpredicted the observed data during this period (Figure 6). This affirms what was visually observed—the upward shift of the observed data after the surfactant reaches the well.

Next, keeping the CV constant and allowing the mass-transfer coefficient to change, the model was calibrated for the next 100 days. The model curve shows that after the first 100 days a greater mass-transfer constant was required to match the later data; the mass-transfer coefficient increases 30% in magnitude ($k = 3.45 \times 10^{-7}\,\mathrm{s}^{-1}$), and the model curve shows an upward shift (Figure 7). This rather abrupt shift in the model curve is not to be expected in reality and is an artifact of the modeling method; moreover, the value of $k = 3.45 \times 10^{-7}\,\mathrm{s}^{-1}$ determined in this model is only an approximate value. To perform accurate modeling, the kinetic parameters would have to be varied as a function of surfactant concentration.

Similarly, for well 92-17 the aqueous TCE data was used to calibrate the kinetic sorption parameters (k and CV). The surfactant took about 6 days from the date of injection to reach this well around day 40. Upon fitting the data for the first 36 days (when there was no surfactant in the system), it is found that the CV was 9.3×10^{-3} and the mean mass-transfer coefficient was $5.74 \times 10^{-7}\,\mathrm{s}^{-1}$. When the model is projected into the next 30 days using these parameters, the model underpredicted the observed data (Figure 8), suggesting that a higher mean mass-transfer constant could be operative in the field in the presence of Triton X-100.

Sensitivity Analysis. Considering the complexity of the modeling, the large number of parameters, and the difficulty in accurately assessing them, it is necessary to determine the sensitivity of the model to these parameters. This will help identify the parameters that are critical to the accuracy of the model. It is especially important to test the sensitivity
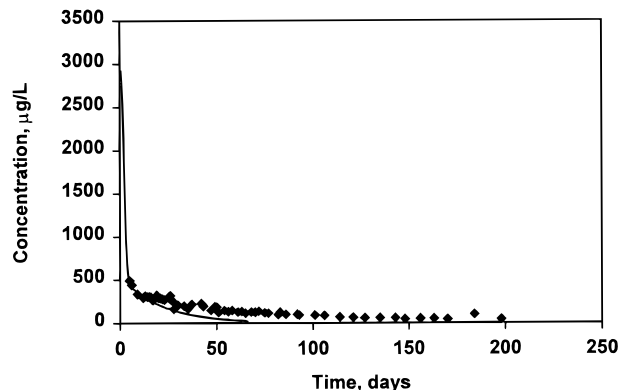

FIGURE 8. Observed and model predicted TCE concentrations (using multisite model) in well 92-17. The model results are based on kinetic rate parameters obtained from fitting the first 36 days TCE data.
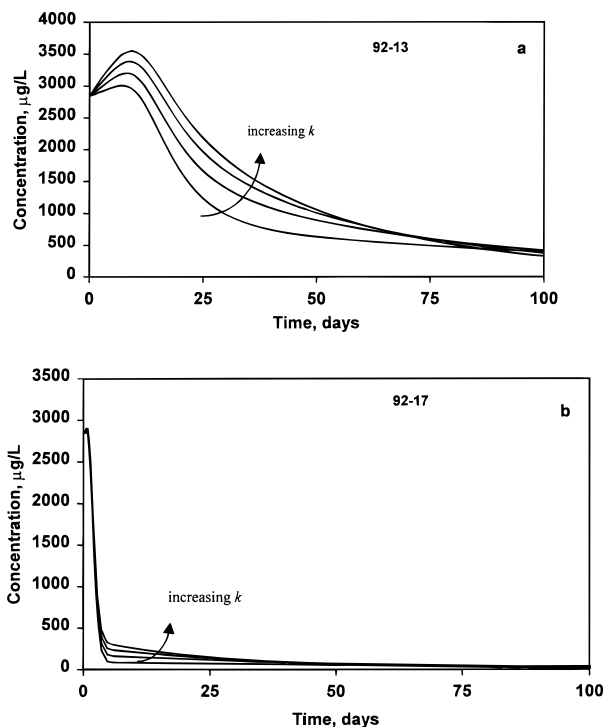

FIGURE 9. Model-predicted TCE concentrations (multisite model) using varying mean rate constants k ($k = 1.0 \times 10^{-7}$, 2.0×10^{-7}, 3.0×10^{-7}, and $4.0 \times 10^{-7}\,\mathrm{s}^{-1}$) in (a) well 92-13 with and in (b) well 92-17.

of the model to those parameters that are difficult to determine with accuracy, such as the kinetic parameters CV and k in the multisite model.

The sensitivity plots for k for wells 92-13 and 92-17 are shown in Figure 9. The sensitivity plots for CV in well 92-13 are shown in Figure 10 (at $k = 1.0 \times 10^{-7}$ and $3.0 \times 10^{-7}\,\mathrm{s}^{-1}$). Table 1 shows the percent errors of the concentration profile at various values of k relative to $k = 1.0 \times 10^{-7}\,\mathrm{s}^{-1}$ and CV $= 0.5$ in well 92-13 and well 92-17. Table 2 shows the percent errors of the concentration profile at various values of the CV relative to a CV of 0.5 at two different k values (1.0×10^{-7} and $3.0 \times 10^{-7}\,\mathrm{s}^{-1}$) in wells 92-13 and 92-17. The percent errors are a measure of deviation from an arbitrary reference model run. Percent error is calculated as $100 \times$ SSD/SSQ; where SSD is the sum of deviation between the two simulated concentrations calculated at the times samples were collected. SSQ is the sum of squares of concentration in the reference model run at those points in time. First, it is seen
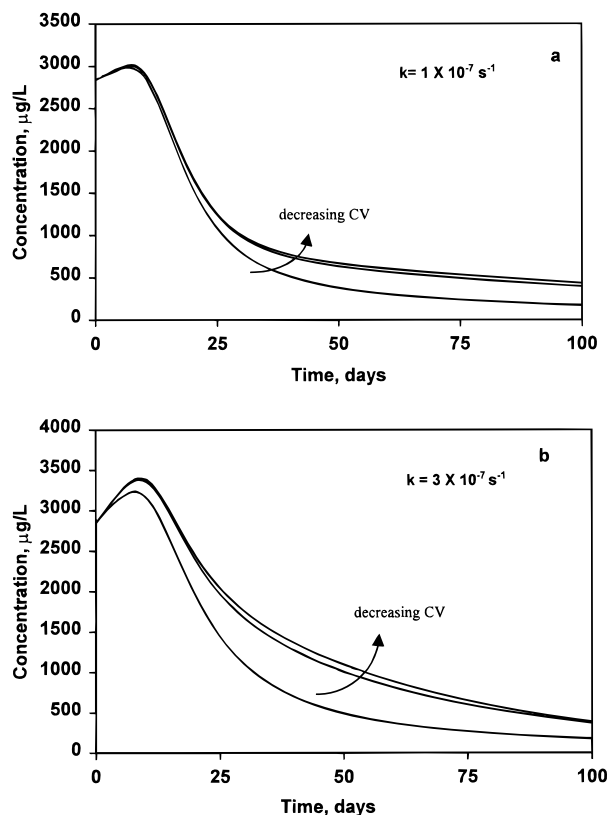
FIGURE 10. Model-predicted TCE concentrations (multisite model) at various CV (CV = 0.0001, 0.5, 2.0) for well 92-13 using (a) mean rate constant $k = 1.0 \times 10^{-7}$ s^{-1} and (b) mean rate constant $k = 3.0 \times 10^{-7}$ s^{-1}.

TABLE 1. Sensitivity of Multisite Model to Variation in Mean Kinetic Rate Constant, k, in Wells 92-13 and 92-17 Given as Percent Error[a] with Respect to Reference Model Run (with Mean $k = 1.0 \times 10^{-7}$ s^{-1})[b]

k (s^{-1})	1.0×10^{-7} (ref value)	2.0×10^{-7}	3.0×10^{-7}	4.0×10^{-7}
percent error (well 92-13)		0.14	0.44	0.81
percent error (well 92-17)		2.40	6.32	10.18

[a] Percent error = 100 × SSD/SSQ. SSD is the sum of deviation between the two simulated concentrations calculated at the times samples were collected. SSQ is the sum of squares of concentration in the reference model run at those points in time. [b] Coefficient of variation is 0.5 for all model runs.

TABLE 2. Sensitivity of Model to Variation in Coefficient of Variation, CV, in Wells 92-13 and 92-17 Given as Percent Error with Respect to Reference Model Run (with CV = 0.5)

CV	mean rate constant = 1.0×10^{-7} s^{-1}			mean rate constant = 1.0×10^{-7} s^{-1}		
	0.0001	0.5 (ref value)	2	0.0001	0.5 (ref value)	2
percent error (well 92-13)	0.026		1.68	0.104		5.90
percent error (well 92-17)	0.002		0.094	0.007		0.28

(Table 1) that the model is more sensitive to k at well 92-17 than it is at well 92-13. This is because of the high flushing rate in 92-17 (relative to 92−13); since advection is strong, k, the mass-transfer constant, is controlling. The sensitivity

to CV is quite low when CV is decreased below 0.5 (Table 2). This implies that below a CV of 0.5 a single mass-transfer coefficient (e.g., a one-site model or a two-site model) could be used.

Model runs for the field show that a significant increase in the mass-transfer coefficient does not translate into a significant increase in the TCE concentration in the wells. From Figure 9a it can be seen that at later times the model is not very sensitive to k. Figure 7 shows that even a significant increase in the mass-transfer coefficient (30%) results in small concentration increases in the wells. This implies that increases (or decreases) in mass-transfer rate coefficients will not result in significantly higher concentrations in the wells. Thus, the effectiveness of Triton X-100 in increasing desorption rate is not expected to be easily observed from the well TCE concentration data.

Summary and Future Work

The data and modeling results from wells 92-13 and 92-17 show consistent evidence of an increase in TCE desorption that is attributable to the presence of Triton X-100. Although visual examination of the concentration profile in the wells does not show any sharp jump in concentration due to surfactant, modeling results show a significant increase in the mass-transfer rate constant. Together, the results from laboratory studies (3) and this field study suggest that Triton X-100 has at least a modest impact on enhancing the desorption rate. It is clear that even the use of surfactant will not result in complete cleanup. However, surfactants may be used to decrease the time that is needed for cleanup to proceed to an acceptable level (e.g., when the aqueous-phase contaminant concentration is brought below regulatory limits).

A few recommendations may be made based on the findings of this and previous studies (3). The partition coefficient (K_d) of TCE varies moderately with Triton X-100 concentration, and its effect on TCE desorption should be considered. The earlier laboratory studies (3) showed the TCE partition coefficient (K_d) increases with Triton X-100 concentration and reaches its highest value at about 500 mg/L of Triton X-100 before decreasing again. For instance, the TCE partition coefficient in a soil−water system is 12% higher at 400 mg/L of Triton X-100 as compared to that at 100 mg/L. Increased K_d slows down the desorption rate by decreasing the concentration gradient (3). A lower surfactant concentration in the field close to or less than the cmc may be more effective and should be tested.

Other surfactants may be more effective in promoting desorption than Triton X-100. In choosing a different surfactant, it should be remembered that a surfactant's ability to influence solute desorption is related to its ability to lower surface tension, its effect on solute sorption coefficient, and the sorption of the surfactant itself onto the soil.

Acknowledgments

Literature Cited

(1) Imbrigiotta, T. E.; Ehlke, T. A.; Martin, M.; Koller, D.; Smith, J. A. *Hydrol. Sci. Technol.* **1995**, *11*, 26−50.
(2) Pignatello, J. J.; Xing, B. *Environ. Sci. Technol.* **1996**, *30*, 1−11.

(3) Sahoo, D.; Smith, J. A. *Environ. Sci. Technol.* **1997**, *31*, 1910−1915.

(4) Smith, J. A.; Chiou, C. T.; Kammer, J. A.; Kile, D. E. *Environ. Sci. Technol.* **1990**, *24*, 676−683.

(5) Culver, T. B.; Hallisey, S. P.; Sahoo, D.; Deitsch, J. J.; Smith, J. A. *Environ. Sci. Technol.* **1997**, *31*, 1581−1588.

(6) Pavlostathis, S. G.; Mathavan, G. N. *Environ. Sci. Technol.* **1992**, *26*, 532−538.

(7) Freyberg, D. L. *Water Resour. Res.* **1986**, *22*, 2031−2046.

(8) Mackay, D. M.; Freyberg, D. L.; Roberts, P. V.; Cherry, J. A. *Water Resour. Res.* **1986**, *22*, 2017−2029.

(9) Schneider, A. D.; Wiese, A. F.; Jones, O. R. *J. Agron.* **1977**, *69*, 432−436.

(10) Curtis, G. P.; Roberts, P. V.; Reinhard, M. *Water Resour. Res.* **1986**, *22*, 2059−2067.

(11) Roberts, P. V.; Goltz, M. N.; Mackay, D. M. *Water Resour. Res.* **1986**, *22*, 2047−2058.

(12) Sudicky, E. A. *Water Resour. Res.* **1986**, *22*, 2069−2082.

(13) Scalf, M. R.; Dunlap, W. J.; Mcmillion, L. G.; Keeley, J. W. *Water Resour. Res.* **1969**, *5*, 1041−1052.

(14) Whiffen, R. B.; Bahr, J. M. *Proceedings of the Fourth National Symposium on Aquifer Restoration and Groundwater Monitoring*; National Water Well Association: Dublin, OH, 1984; pp 75−81.

(15) Chiou, C. T.; Peters, L. J.; Freed, V. H. *Science* **1979**, *206*, 831−832.

(16) Weber, W. J.; Huang, W. *Environ. Sci. Technol.* **1996**, *30*, 881−888.

(17) Brusseau, M. L.; Rao, P. S. C. *Crit. Rev. Environ. Control* **1989**, *19*, 33−88.

(18) Deitsch, J. J.; Smith, J. A. *Environ. Sci. Technol.* **1995**, *29*, 1069−1080.

(19) Carroll, K. M.; Harkness, M. R.; Bracco, A. A.; Balcarcel, R. R. *Environ. Sci. Technol.* **1994**, *28*, 253−258.

(20) Yeom, I. T.; Ghosh, M. M.; Cox, C. D. *Environ. Sci. Technol.* **1996**, *30*, 1589−1595.

(21) deGennes, P. G. Cornell University Press: Ithaca, 1979.

(22) DiCesare, D.; Smith, J. A. *Rev. Environ. Contam. Toxic* **1994**, *134*.

(23) Cussler, E. L. *Diffusion: Mass transfer in Fluid Systems*; Cambridge University Press: Cambridge, UK, 1984.

(24) Frisch, H. L. *Polym. Eng. Sci.* **1980**, *20*, 2−13.

(25) Okuda, I.; Mcbride, J. F.; Gleyzer, S. N.; Miller, C. T. *Environ. Sci. Technol.* **1997**, *30*, 1852−1860.

(26) Smith, J. A.; Sahoo, D.; McLellan, H.; Imbrigiotta, T. *Environ. Sci. Technol.* **1997**, *31*, 3565−3572.

(27) Smith, J. A.; Cho, H. J.; Jaffe, P. R.; MacLeod, C. L.; Koehnlein, S. A. *J. Environ. Qual.* **1992**, *21*, 264−271.

(28) Smith, J. A.; Tisdale, A. K.; Cho, H. J. *Environ. Sci. Technol.* **1996**, *30*, 2243−2250.

(29) Sargent, B. P.; Fusillo, T. V.; Storck, D. A.; Smith, J. A. *Water Resources Investigation Report 90-4057*; U.S. Geological Survey: Washington, DC, 1990.

(30) Imbrigiotta, T. E.; Martin, M. In *U.S. Geological Survey Toxic Substances Hydrology Program*−Proceedings of the Technical Meeting, Monterey, CA, March 11−15, 1991; Mallard, G. E., Aronson, D. A., Eds.; Water-Resources Investigations Report 91-4034; U.S. Geological Survey: Washington, DC, 1991; Vol. 91, pp 673−680.

(31) Cho, H. J.; Jaffe, P. R.; Smith, J. A. *Water Resour. Res.* **1993**, *29*, 3329−3342.

(32) Imbrigiotta, T. E.; Martin, M. In *U.S. Geological Survey Toxic Substances Hydrology Program*−Proceedings of the Technical Meeting, Colorado Springs, CO, September 20−24, 1993; Morganwalp, D. W., Aronson, D. A., Eds.; Water-Resources Investigations Report 94-4015; U.S. Geological Survey: Washington, DC, 1996; pp 297−306.

(33) Crabb, N. T.; Persinger, H. E. *J. Am. Oil Chem. Soc.* **1964**, *41*, 752−755.

(34) Greff, R. A.; Setzkorn, E. A.; Leslie, W. D. *Journal of the American Oil Chemists' Society* **1965**, *42*, 180−185.

(35) Sawhney, B. L.; Pignatello, J. J.; Steinberg, S. M. *J. Environ. Qual.* **1988**, 149−152.

(36) Press: W. H.; Flannery, B. P.; Teukolsky, S. A.; Vetterling, W. T. *Numerical Recipes*; Cambridge University Press: Cambridge, 1986.

(37) Bahr, J. M. Ph.D. Dissertation, Stanford University, Palo Alto, CA, 1989.

(38) Valocchi, A. J. *Water Resour. Res.* **1989**, *5*, 273−279.

(39) Cvetkovic, V. D.; Shapiro, A. M. *Water Resour. Res.* **1990**, *26*, 2057−2067.

(40) Voss, C. I. *Water Resour. Invest.* (*U.S. Geol. Surv.*) **1984**, *No. 84-4369*.